constants from multiple-time uptake data. Generalizations. *J Cereb Blood Flow Metab* 1985;5:584–590.
31. Landaw EM, DiStefano JJ. Multiexponential, multicompartmental non-compartmental modeling. II. Data analysis and statistical considerations. *Am J Physiol* 1984;246:R665–R677.
32. Hosking DJ and Chamberlain MJ. Studies in man with ^{18}F. *Clin Sci* 1972;42:153–161.
33. Simonet WT, Bronk JT, Pinto MR, Williams EA, Meadows TH, Kelly PJ. Cortical and cancellous bone: age-related changes in morphological features, fluid spaces, and calcium homeostasis in dogs. *Mayo Clin Proc* 1988;63:154–160.
34. Li G, Bronk, JT, Kelly PJ. Canine bone blood flow estimated with microspheres. *J Ortho Res* 1989;7:61–67.
35. Kalender WA, Felsenberg D, Louis O, et al. Reference values for trabecular and cortical vertebral bone density in single- and dual-energy quantitative computed tomography. *Eur J Rad* 1989;9:75–80.

SELF-STUDY TEST

Skeletal Nuclear Medicine

Questions are taken from the *Nuclear Medicine Self-Study Program I*, published by The Society of Nuclear Medicine

DIRECTIONS

The following items consist of a question or incomplete statement followed by five lettered answers or completions. Select the *one* lettered answer or completion that is *best* in each case. Answers may be found on page 747.

1. The "flare" phenomenon in bone scintigraphy refers to which *one* of the following?

- **A.** An increase in uptake in healing metastases following therapy
- **B.** The extended pattern seen with primary bone tumors.
- **C.** The flame-like edge seen in long-bone lesions of Paget's disease.
- **D.** The persisting minimal uptake seen in regressing metastases.
- **E.** The calvarial flame seen in the skull on oblique views.

2. Which *one* of the following mechanisms is most important in causing locally increased uptake of a bone-seeking radiopharmaceutical in an osseous lesion?

- **A.** Increased blood flow
- **B.** Increased compact bone mass
- **C.** The presence of excessive organic matrix
- **D.** Increased local alkaline phosphatase activity
- **E.** Increased surface area of hydroxyapatite crystals per unit volume of bone

3. A bone mineral measurement on the lumbar spine of a middle-aged woman was performed by dual-photon absorptiometry. Areal density was 0.75 g/cm². This value is below the fracture threshold of 0.98 g/cm² and below the second percentile of the normal range, based on age, race, and sex-matched controls. The bone mineral image from which the quoted results were obtained is shown in Figure 1. Which *one* of the following statements regarding the interpretation of the bone mineral measurements in this patient is correct?

- **A.** The bone mineral image shows evidence for significant degenerative disease.
- **B.** The tracing shows some bone mineral in the location of the transverse processes. This invalidates the results and a radial bone mineral measurement should be used, instead, for evaluation of this patient.
- **C.** Nearly all women with a bone mineral value of 0.75 g/cm² have one or more compression fractures.
- **D.** The bone mineral measurement is likely to be of no clinical significance in this patient.
- **E.** The bone mineral image shows uniform bone mineral distribution in the lumbar spine.

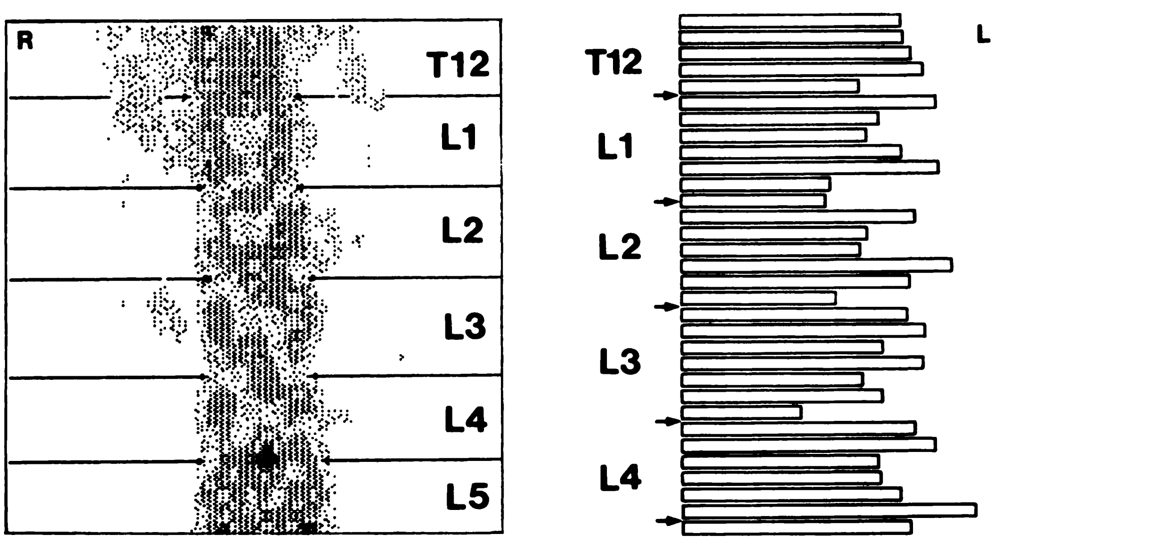

Figure 1

(continued on page 683)

pulmonary embolism. *Circulation* 1969;39:663–674.
20. Wellman HN, Mack JF, Saenger EL, Friedman BI. Clinical experience with oblique views in pulmonary perfusion scintigraphy in normal and pathological anatomy. *J Nucl Med* 1968;9:374.
21. Surprenant EL, Browning N, Webber MM. The significance of shine-through on the side view lung scan. *J Nucl Med* 1967;8:400.
22. Foster-Carter AF. The anatomy of the bronchial tree. *Br J Tuberculosis* 1942;36:19–39.
23. Brock RC. *The anatomy of the bronchial tree*, 2nd edition. London: Oxford University Press; 1954.
24. Anderson JE. *Grant's atlas of anatomy*, 7th edition. London: Williams and Wilkins; 1980.
25. Terry PB, Traystman RJ, Newball HH, et al. Collateral ventilation in man. *N Engl J Med* 1978;298:10–15.
26. Berg RM, Boyden EA, Smith FR. An analysis of the segmental bronchi of the left lower lobe of fifty dissected, and ten injected, lungs. *J Thorac Surg* 1949;18:216–236.
27. Ceraldi CM, Schabel SI, Waxman K. Normal ventilation/perfusion lung scan in a patient with proven pulmonary embolus. *Crit Care Med* 1990; 18:577–578.

(continued from page 642)

SELF-STUDY TEST

4. This 66-yr-old man with known chronic lymphocytic leukemia has pain in his left thigh and low-grade fever. You are shown an anterior image from a ^{99m}Tc MDP bone scan (Fig. 2) and anterior and left lateral images obtained with ^{67}Ga citrate (Fig. 3.) Which *one* of the following is the best explanation for the focal abnormality (arrow) in the left femur?

- **A.** Acute osteomyelitis
- **B.** Acute infarct
- **C.** Chronic infarct
- **D.** Leukemic infiltration
- **E.** Metastatic carcinoma

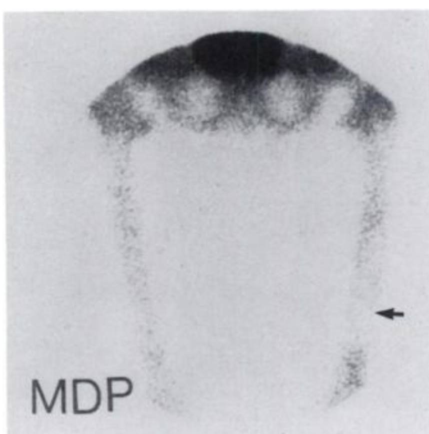

R Ant L

Figure 2

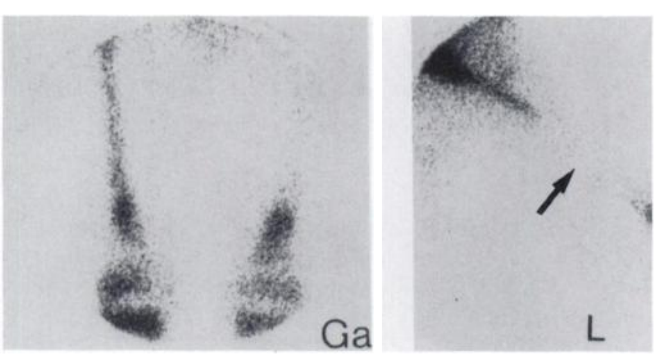

R Ant L Lat

Figure 3

5. This 58-yr-old woman has had pain and swelling of the right hand for several weeks. You are shown images from three-phase skeletal scintigraphy with ^{99m}Tc MDP (Fig. 4). Which *one* of the following is the most likely diagnosis?

- **A.** Rheumatoid arthritis
- **B.** Calcium pyrophosphate dihydrate (CPPD) crystal deposition disease
- **C.** Reflex sympathetic dystrophy syndrome
- **D.** Cellulitis
- **E.** Post-traumatic arteriovenous fistula

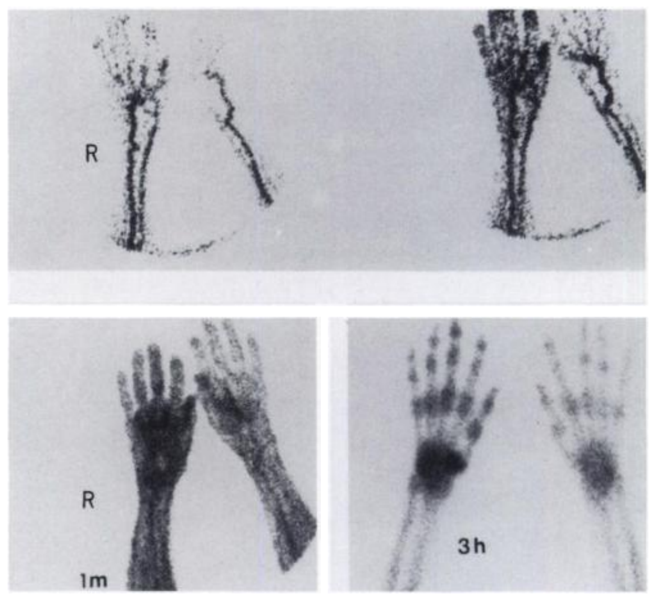

Figure 4

6. Which *one* of the following is the *least* likely scintigraphic finding expected with a 1-wk-old, uncomplicated fracture?

- **A.** Increased perfusion at the fracture site on radionuclide angiography with ^{99m}Tc MDP.
- **B.** Increased "blood-pool" activity at the fracture site on an immediate image with ^{99m}Tc MDP.
- **C.** Increased concentration of ^{99m}Tc MDP at the fracture site on a 3-hr delayed image.
- **D.** Increased uptake of ^{67}Ga citrate at the fracture site.
- **E.** Increased uptake of ^{111}In-labeled leukocytes at the fracture site.

(continued on page 747)

REFERENCES

1. Yamada R, Sato M, Kawabata M, Nakatsuka H, Nakamura K, Kobayashi N. Segmental obstruction of the hepatic inferior vena cava treated by transluminal angioplasty. *Radiology* 1983;149:91–96.
2. Meier WL III, Waller RM III, Sones PJ Jr, et al. Budd-Chiari web treated by percutaneous transluminal angioplasty. *AJR* 1981;137:1257–1258.
3. Shiomi S, Kuroki T, Ueda T, et al. Significance of blood flow in the inferior and superior mesenteric veins for the formation of oesophageal varices. *J Gastroenterol Hepatol* 1991;6:151–154.
4. McDermott WV, Stone MD, Bothe A, Jr. Budd-Chiari syndrome. Historical and clinical review with an analysis of surgical corrective procedures. *Am J Surg* 1984;147:463–467.
5. Koizumi M, Sekine M, Imazuki S, Kawamura T, Iio A, Hamamoto K. RI venography of membranous obliteration of the inferior vena cava in the hepatic portion. *Jpn J Clin Radiol* 1984;29:1419–1422.
6. Ohtomo K, Furui S, Kokubo T, Yashiro N, Itai Y, Iio M. CT diagnosis of membranous obstruction of the hepatic segment of the inferior vena cava (primary Budd-Chiari syndrome). *Jpn J Clin Radiol* 1987;32:275–279.
7. Halkar RK. Budd-Chiari syndrome. *Radiology* 1989;172:580.
8. Tavill AS, Wood EJ, Kreel L, Jones EA, Gregory M, Sherlock S. The Budd-Chiari syndrome: correlation between hepatic scintigraphy and the clinical, radiological, and pathological findings in nineteen cases of hepatic venous outflow obstruction. *Gastroenterology* 1975;68:509–518.
9. Lee VW, Peng TT, O'Brien MJ, Hauck RM. Budd-Chiari syndrome complicating hepatocellular carcinoma demonstration by multiple radiotracer scintigraphy. *Clin Nucl Med* 1986;11:102–107.
10. Sy WM, Lao RS, Nissen A, Kim TS. Occlusion of inferior vena cava: features by radionuclide venography. *J Nucl Med* 1978;19:1007–1012.
11. Huang M-J, Liaw Y-F, Tzen K-Y. Radionuclide venography in Budd-Chiari syndrome with intrahepatic vena caval obstruction. *J Nucl Med* 1985;26:145–148.

(continued from page 683)

SELF-STUDY TEST
Skeletal Nuclear Medicine
ANSWERS

ITEM 1: "Flare" Phenomenon

ANSWER: A

The term "flare phenomenon" was originally used by Gillespie et al. to describe the increase in activity seen on ^{87m}Sr bone scans during treatment of patients with metastatic disease who were responding to chemotherapy. This phenomenon was further characterized by Rossleigh et al. in patients undergoing ^{99m}Tc MDP bone scintigraphy for evaluation of therapy for breast cancer metastases. They defined the "flare response" as: (1) an increase in tracer uptake or in the apparent size of known metastatic lesions and/or the appearance of new lesions within 6 mo of commencing therapy, in the absence of increasing bone pain (in practice, however, pain occurs in some patients responding to therapy); and (2) subsequent decreased uptake in these lesions, without a change in therapy, on repeat scintigraphy within 2–3 mo. In this series, ten patients showed a healing "flare response" 6 wk to 6 mo after therapy. Five of the ten patients showed increased uptake in previously demonstrated lesions. In the other five patients, new lesions were identified that previously were undetected. In all of the patients, therapy was not altered during the course of the serial studies, there was a reduction in bone pain or objective tumor responses in other sites, and later follow-up studies showed decreased uptake in the known lesions. In only one of the patients was a radiographic change (sclerosis of a lytic lesion) seen in association with the healing flare. The "flare phenomenon" has been seen in patients with prostate carcinoma and other tumors, as well. It also may occur locally in regions undergoing irradiation for metastatic disease. The likelihood of observing the "flare phenomenon" depends on the type of tumor, the type of therapy, the interval after onset of treatment, and the frequency of bone scintigraphy.

The "extended pattern" seen with primary bone tumors in long bones is not related to the "flare phenomenon." Patients with primary bone tumors may show increased activity in adjacent joints or along the entire extremity. This increase in activity is usually mild to moderate in degree and is thought to be due either to generalized increased blood flow to the extremity or to a change in the patient's gait. The "extended pattern" is one reason that bone scintigraphy may overestimate the extent of osseous involvement by a primary bone tumor. Similar "extended" findings also occur with inflammatory lesions of the long bones.

When Paget's disease involves long bones, the process may involve the entire bone or it may extend from one end of the bone for a variable length into the diaphysis. Radiographically, the leading edge of the lytic phase of Paget's disease in a long bone has been described as a "flame-like" rarefaction. This also has been characterized as a "blade of grass" appearance.

The persisting minimal uptake seen in regressing metastases is not the "flare phenomenon." This uptake likely reflects continued remodeling of bone after the local tumor deposit has been reduced or eradicated.

On oblique scintigrams of the skull, an area of increased activity in the anterior temporoparietal region is occasionally seen. This has been called a calvarial flame and probably is due to the increased bone thickness of the lateral orbital ridge or the pterion viewed on end in this projection.

References

1. Gillespie PJ, Alexander JL, Edlestyn GA. Changes in ^{87m}Sr concentrations in skeletal metastases in patients responding to cyclical combination chemotherapy for advanced breast cancer. *J Nucl Med* 1975;16:191–193.
2. Goldman AB, Braunstein P. Augmented radioactivity on bone scans of limbs bearing osteosarcomas. *J Nucl Med* 1975;16:423–424.
3. Levenson RM, Sauerbrunn BJL, Bates HR, Newman RD, Eddy JL, Ihde DC. Comparative value of bone scintigraphy and radiography in monitoring tumor response in systemically treated prostatic carcinoma. *Radiology* 1983;146:513–518.
4. Pollen JJ, Witztum KF, Ashburn WL. The flare phenomenon on radionuclide bone scan in metastatic prostate cancer. *AJR* 1984;142:773–776.
5. Rossleigh MA, Lovegrove FTA, Reynolds PM, Byrne MJ, Whitney BP. The assessment of response to therapy of bone metastases in breast cancer. *Aust NZ J Med* 1984;14:19–22.
6. Thrall JH, Geslien GE, Corcoron RJ, Johnson MC. Abnormal radionuclide deposition patterns adjacent to focal skeletal lesions. *Radiology* 1975;115:659–663.

ITEM 2: Mechanisms of Radiopharmaceutical Uptake in Osseous Lesions

ANSWER: E

Bone-seeking radiopharmaceuticals are accumulated in greater degree at skeletal sites where there is increased blood flow (thus exposing that bone to more tracer for chemisorption over any given time), and also in sites of new bone formations where there is an increase in the surface area of hydroxyapatite crystals per unit volume of bone. Newly forming hydroxyapatite crystals are of smaller size than mature crystals and provide a relatively greater surface area for chemisorption of the tracer. Although both increased blood flow and new bone formation (with associated increase in crystal surface area) are important, several studies have shown that the magnitude of the change in blood flow is insufficient to account for the substantially increased tracer accumulation in epiphyseal plates, metastatic lesions, and healing fractures.

A large mass of compact bone with normal blood flow and hydroxyapatite deposition will not necessarily have increased uptake; e.g., bone islands are not usually noticeably "hot" by scintigraphy.

The organic matrix has rather low affinity for the ^{99m}Tc diphosphonate agents when compared with hydroxyapatite crystals. There is little experimental evidence that alkaline phosphatase activity bears a relationship to the localization of bone-seeking radiopharmaceuticals.

References

1. Charkes ND. Skeletal blood flow: implications for bone-scan interpretation. *J Nucl Med* 1980;21:91–98.
2. Fogelman I. Skeletal uptake of diphosphonate: a review. *Eur J Nucl Med* 1980;5:473–476.
3. Francis MD, Ferguson DL, Tofe AJ, Bevan JA, Michaels SE. Competitive evaluation of three diphosphonates: in vitro adsorption (C-14 labeled) and in vivo osteogenic uptake (Tc-99m complexed). *J Nucl Med*1980;21:1185–1189.
4. Hughes SPF, Davies DR, Bassingthwaighte JB, Knox FG, Kelly PJ. Bone extraction and blood clearance of diphosphonate in the dog. *Am J Physiol* 1977;232:H341–H347.

(continued on page 770)

12. Cerqueira MD, Harp GD, Ritchie JL, Stratton JR, Walker RD. Rarity of preclinical alcoholic cardiomyopathy in chronic alcoholics <40 years of age. *Am J Cardiol* 1991;67:183–187.
13. Budinger TF, Gullberg GT, Huesman RH. *Topics in applied physics: image reconstruction from projections, volume 32.* New York: Springer-Verlag; 1979:197–199.
14. Sinusas AJ, Beller GA, Smith WH, Vinson EL, Brookeman V, Watson DD. Quantitative planar imaging with technetium-99m-methoxyisobutyl isonitile: comparison of uptake patterns with thallium-201. *J Nucl Med* 1989;30:1456–1463.
15. Koster K, Wackers FJT, Mattera JA, Fetterman RC. Quantitative analysis of planar technetium-99m-sestamibi myocardial perfusion images using modified background subtraction. *J Nucl Med* 1990;31:1400–1408.
16. Grenier R, Port S. Geometric methods for determining left ventricular volume [Reply]. *J Nucl Med* 1991;32:553–555.
17. Sandler H, Dodge HT. The use of single plane angiocardiograms for the calculation of left ventricular volume in man. *Am Heart J* 1968;75:325–334.
18. Laskey WK, John Sutton M, Zeevi G, Hirshfeld JW, Reichek N. Left ventricular mechanics in dilated cardiomyopathy. *Am J Cardiol* 1984;54:620–625.
18. Hotelling H. The selection of variates for use in prediction with some comments on the general problem of nuisance parameters. *Ann Math Stat* 1940;11:271–283.
20. Moss AJ, et al. Risk stratification and survival after myocardial infarction. *N Engl J Med* 1983;309:331–336.
21. Lee LL, Pryor DB, Pieper KS, et al. Prognostic value of radionuclide angiography in medically treated patients with coronary artery disease. *Circulation* 1990;82:1705–1717.
22. White HD, Norris RM, Brown MA, et al. Left ventricular end-systolic volume is the major determinant of survival after recovery from myocardial infarction. *Circulation* 1987;76:44–51.
23. Henry WL, Bonow RO, Borer JS, et al. Observations on the optimum time for operative intervention for aortic regurgitation. I. Evaluation of the results of aortic valve replacement in symptomatic patients. *Circulation* 1980;61:471–483.
24. Henry WL, Bonow RO, Rosing DR, Epstein SE. Observations on the optimum time for operative intervention for aortic regurgitation. II. Serial echocardiographic evaluation of asymptomatic patients. *Circulation* 1980;61:484–492.
25. Neumann P, Schicha H, Schurnbrand P, Bahre M, Emrich D. Visualizing cardiac blood pool: comparison of three labeling methods. *Eur J Nucl Med* 1983;8:463–466.
26. Starling MR, J Dell'Italia LJ, Nusynowitz ML, Walsh RA, Little WC, Benedetto AR. Estimates of left-ventricular volumes by equilibrium radionuclide angiography: importance of attenuation correction. *J Nucl Med* 1984;25:14–20.
27. Dodge HT, Sandler H, Ballew DW, Lord JD. The use of biplane angiocardiography for the measurement of left ventricular volume in man. *Am Heart J* 1960;60:762–776.
28. Sheehan FH, Mitten-Lewis S. Factors influencing accuracy in left ventricular volume determination. *Am J Cardiol* 1989;64:661–664.

(continued from page 747)

SELF-STUDY TEST
Skeletal Nuclear Medicine

ANSWERS

5. Lavender JP, Khan RAA, Hughes SPF. Blood flow and tracer uptake in normal and abnormal canine bone: comparison with Sr-85 microspheres, Kr-81m, and Tc-99m MDP. *J Nucl Med* 1979;20:413–418.
6. McInnis JC, Robb RA, Kelly PJ. The relationship of bone blood flow, bone tracer deposition, and endosteal new bone formation. *J Lab Clin Med* 1980;96:511–522.
7. Siegel BA, Donovan RL, Alderson PO, Mack GR. Skeletal uptake of ^{99m}Tc-diphosphonate in relation to local bone blood flow. *Radiology* 1976;120:121–123.
8. Vattimo A, Martini G, Pisani M. Bone uptake of ^{99m}Tc-MDP in man: its relationship with local blood flow. *J Nucl Med Allied Sci* 1982;26:173–179.

ITEM 3: Interpretation of Lumbar Bone Mineral Measurements
ANSWER: E

When significant degenerative hypertrophic changes are present, or when markedly calcified plaques in the aorta overlie the spine, the measured bone mineral does not accurately reflect bone density in the vertebrae alone and cannot be used to draw diagnostic conclusions regarding bone mass or fracture risk. Other conditions interfering with measurement of spinal bone mass are listed in Table I. Most of the time, these can be identified from the spinal radiographs obtained before the test. Occasionally, however, these problems first become apparent when the bone mineral image is being reviewed.

The tracing depicted in Figure 1 is of good quality and shows no evidence of degenerative disease, spinal deformity, artifacts, or technical problems. There is a uniform distribution of bone mineral in this patient's lumbar spine.

Although the bone mineral images occasionally show bone mineral in the region of the transverse processes on some types of instruments, the processing algorithm eliminates these areas. Further, a manual override is available to allow checking and correcting of the edges if necessary. The image can be displayed with the edges identified for final assessment. In this patient, this would not be necessary.

Less than half of all women with bone mineral values of 0.75 g/cm² have a spinal compression fracture (Table 2). This statistic stresses the distinction between the assessment of fracture risk by bone mineral measurements and the diagnosis of fracture or other irreversible changes by radiography.

Bone mineral assessment is the only nontraumatic test that can be used to measure bone mass in patients at high risk of bone loss prior to the occurrence of irreversible changes. Also, in patients with compression fractures, the amount of bone mass actually present and the risk for further fractures can be assessed only by bone mineral meas-

TABLE 1
False Results in Bone Mineral Measurements

Conditions resulting in falsely high bone mineral
- Marked aortic calcification
- Hypertrophic degenerative joint and disc disease
- Bone grafts
- Lipiodol in the spinal canal
- Calcium-containing tablets in the gastrointestinal tract

Conditions resulting in falsely low bone mineral
- Laminectomy

Conditions resulting in falsely high or low bone mineral
- Compression fractures and other post traumatic changes
- Marked scoliosis and other spinal deformities
- Focal vertebral lesions (lytic or sclerotic)

[Table 1 adapted from Freeman LM, Weissmann HS, eds, *Nuclear Medicine Annual 1986*. Raven Press, 1986:195–226.]

TABLE 2
Relationship Between Bone Mineral and Fracture Risk in Normal Women from Minnesota

Bone mineral in spine or femur (g/cm²)	Prevalence of L1–L4 vertebral fractures (%)	Proximal femoral fracture incidence per 1000 person-years: Neck	Trochanter
>1.40	0	0	0
1.20–1.39	0.1	0	0
1.00–1.19	6.8	0.2	0.1
0.80–0.99	26.1	2.0	0.8
0.60–0.79	47.5	6.5	5.3
<0.60	48.8	8.8	17.6

[Table 2 adapted from Wahner HW. Single- and dual-photon absorptiometry in osteoporosis and osteomalacia. *Semin Nucl Med* 1987;17:305–315.]

(continued on page 776)

bilities suitable for imaging ^{131}I therapy patients using absorber sheets. Nonetheless, it is important that any gamma camera system proposed for use in imaging therapeutic levels of ^{131}I be carefully evaluated to determine its count-rate limitations.

The requirement of reducing camera count rates with absorber sheets has prevented us from performing SPECT imaging of therapeutic doses. Although not impossible, SPECT imaging could be cumbersome with the technique we have outlined because the camera system must be able to accurately rotate the additional weight. Other engineering problems include designing a safe method of attaching Pb sheets weighing from 30 to 50 pounds to the front face of the collimator.

There are well known limitations to planar imaging methods of estimating in vivo radiotracer concentrations (*13,14*). However, for relative comparison of radiotracer concentrations in multiple studies of the same subject, planar imaging can be precise (*14*). A comparison of the biodistribution of trace and therapeutic levels of ^{131}I-labeled monoclonal antibodies can be accomplished in this manner. The use of this therapeutic imaging technique will enable us to increase our understanding of radioimmunotherapy dosimetry and patient response to treatment.

ACKNOWLEDGMENTS

The authors thank Ray Thomas, Shelley Hartnett and Marc Milrod for technical assistance. We also appreciate the comments of anonymous reviewers in preparation of this manuscript. This work was supported in part by NIH grants CA42593 and CA47430.

REFERENCES

1. Larson SM. Lymphoma, melanoma, colon cancer: diagnosis and treatment with radiolabeled monoclonal antibodies. *Radiology* 1987;165:297–304.
2. DeNardo SJ, DeNardo GL, O'Grady LF, et al. Treatment of B-cell malignancies with I-131 Lym-1 monoclonal antibodies. *Int J Cancer* 1988; 3(suppl):96–101.
3. Carrasquillo JA, Larson SM. Radioimmunoscintigraphy of lymphoma with monoclonal antibodies. *Cancer Treat Res* 1988;38:209–222.
4. Eary JF, Press OW, Badger CC, et al. Imaging and treatment of B-cell lymphoma. *J Nucl Med* 1990;31:1257–1268.
5. Press OW, Eary JF, Badger CC, et al. Treatment of refractory non-Hodgkin's lymphoma with radiolabeled MB-1 (anti-CD37)antibody. *J Clin Oncol* 1989;7:1027–1038.
6. Lewellen TK, Bice AN, Pollard KR, Zhu JB, Plunkett ME. Evaluation of a clinical scintillation camera with pulse-tail extrapolation electronics. *J Nucl Med* 1989;30:1554–1558.
7. Lewellen TK, Pollard KR, Bice AN, Zhu JB. A new clinical scintillation camera with pulse-tail extrapolation electronics. *IEEE Trans Nucl Sci* 1990;37:702–706.
8. Muehllehner G, Jaszczak RJ, Beck RN. The reduction of coincidence loss in radionuclide imaging cameras through the use of composite filters. *Phys Med Biol* 1974;19:504–510.
9. Pillay M, Shapiro B, Cox PH. The effect of an alloy filter on gamma camera images. *Eur J Nucl Med* 1986;12:293–295.
10. Wiarda KS. Use of a copper filter for dose-calibrator measurements of nuclides emitting K x-rays. *J Nucl Med* 1984;25:633–634.
11. Performance measurements of scintillation cameras. NEMA Standards Publication NU1-1986, 1986.
12. Product data, 3-190. Collimators for GE high-performance XC/T imaging detector. GE Medical Systems, Milwaukee, WI, 1990.
13. Bice AN, Eary JF, Nelp WB. Quantification of iodine-131 distribution by gamma camera imaging. *Eur J Nucl Med* 1991;18:142–143.
14. Eary JF, Appelbaum FL, Durack L, Brown P. Preliminary validation of the opposing view method for quantitative gamma camera imaging. *Med Phys* 1989;16:382–387.

(continued from page 770)

SELF-STUDY TEST ANSWERS

urements. In this patient, a rather unexpectedly low bone mass was found that warrants consideration of an aggressive treatment plan. Other metabolic bone diseases need to be excluded in this patient.

Reference

1. Wahner HW. Bone mineral measurements. In: Freeman LM, Weissmann HS, eds. *Nuclear Medicine Annual 1986*. New York: Raven Press, 1986:195–226.
2. Wahner HW. Single- and dual-photon absorptiometry in osteoporosis and osteomalacia. *Semin Nucl Med* 1987;17:305–315.

ITEM 4: Acute Infarct of Bone

ANSWER: B

The images illustrate typical findings of acute infarction of the left femoral diaphysis in this 66-yr-old man. The scintigraphic studies were ordered to determine whether infection was the cause of bone pain and tenderness. The finding of decreased activity with both ^{99m}Tc and ^{67}Ga virtually excludes the possibility of infection. On bone scintigraphy alone, however, early acute osteomyelitis occasionally appears as a photon-deficient lesion because of interruption of the blood supply to the infected bone.

Chronic infarction and metastatic carcinoma generally are associated with enhanced ^{99m}Tc MDP uptake. The uptake of ^{67}Ga in a region of chronic infarction is variable, but will be less than that seen with ^{99m}Tc MDP. Depending on the specific carcinoma, ^{67}Ga uptake in a metastasis that was photon-deficient on bone scintigraphy would likely be increased because of gallium accumulation in the tumor tissue. Bone scintigraphy in uncomplicated leukemia (particularly chronic leukemia) is normal, but increased activity may be seen if there is cellular packing of the medullary cavity. In children with acute leukemia, focal metaphyseal lesions resembling metastases may be seen. Also, in acute leukemia, ^{67}Ga scintigraphy often shows a generalized increase in skeletal accumulation of tracer, but the appearance is more often normal with chronic leukemias.

References

1. Amundsen TR, Siegel MJ, Siegel BA. Osteomyelitis and infarction in sickle cell hemoglobinopathies: differentiation by combined technetium and gallium scintigraphy. *Radiology* 1984;153:807–812.
2. Armas RR, Goldsmith SJ. Gallium scintigraphy in bone infarction. Correlation with bone imaging. *Clin Nucl Med* 1984;9:1-3.
3. Bekerman C, Hoffer PB, Bitran JD. The role of gallium-67 in the clinical evaluation of cancer. *Semin Nucl Med* 1984;14:296–323.

ITEM 5: Reflex Sympathetic Dystrophy Syndrome

ANSWER: C

The three-phase scintigraphic study in Figure 4 demonstrates marked diffuse hyperperfusion and hyperemia of the right hand and wrist. There is moderate diffusely increased activity on the delayed image with periarticular accentuation. These findings are characteristic of the reflex sympathetic dystrophy syndrome (Sudek's atrophy). Among the listed options, cellulitis is the most difficult to exclude. The hyperperfusion and hyperemia would be typical findings with cellulitis but, in general, the delayed images will show only a mildly diffuse increase in tracer accumulation in the subjacent bone or bones. The presence of symptoms for several weeks also would be atypical for cellulitis; affected patients usually seek medical attention sooner than this.

It would be most unusual for acute rheumatoid synovitis to involve all

(continued on page 818)

man AJ, Boucher CA, Strauss HW. Comparison of thallium redistribution with rest "reinjection" imaging for detection of viable myocardium. *Am J Cardiol* 1990;66:158-163.
35. Tamaki N, Ohtani H, Yonekura Y, et al. Significance of fill-in after thallium-201 reinjection following delayed imaging: comparison with regional wall motion and angiographic findings. *J Nucl Med* 1990;31:1617-1623.
36. Ohtani H, Tamaki N, Yonekura Y, et al. Value of thallium-201 reinjection after delayed SPECT imaging for predicting reversible ischemia after coronary artery bypass grafting. *Am J Cardiol* 1990;66:394-399.
37. Kayden DS, Sigal S, Soufer R, Mattera J, Zaret BL, Wackers FThJ. Thallium-201 for assessment of myocardial viability: quantitative comparison of 24-hour redistribution imaging with imaging after reinjection at rest. *J Am Coll Cardiol* 1991;18:1480-1486.
38. Dilsizian V, Freedman NMT, Bacharach SL, Perrone-Filardi P, Bonow RO. Regional thallium uptake in irreversible defects: magnitude of change in thallium activity after reinjection distinguishes viable from nonviable myocardium. *Circulation* 1992;85:627-634.
39. Bonow RO, Dilsizian V, Cuocolo A, Bacharach SL. Identification of viable myocardium in patients with chronic coronary artery disease and left ventricular dysfunction: comparison of thallium-201 with reinjection and PET imaging with ^{18}F-fluorodeoxyglucose. *Circulation* 1991; 83:26-37.
40. Tamaki N, Ohtani H, Yamashita K, et al. Metabolic activity in the areas of new fill-in after thallium-201 reinjection: comparison with positron emission tomography using fluorine-18-deoxyglucose. *J Nucl Med* 1991;32: 673-678.
41. Tillisch JH, Brunken R, Marshall R, et al. Reversibility of cardiac wall-motion abnormalities predicted by positron tomography. *N Engl J Med* 1986;314:884-888.
42. Rocco TP, Dilsizian V, Strauss HW, Boucher CA. Technetium-99m isonitrile myocardial uptake at rest. II. Relation to clinical markers of potential viability. *J Am Coll Cardiol* 1989;14: 1678-1684.
43. Taillefer R, Primeau M, Costi P, Lambert R, Leveille J, Latour Y. Technetium-99m-sestamibi myocardial perfusion imaging in detection of coronary artery disease: comparison between initial (1-hour) and delayed (3-hour) postexercise images. *J Nucl Med* 1991;32:1961-1965.
44. Sinusas AJ, Bergin JD, Edwards NC, Watson DD, Ruiz M, Beller GA. Technetium-99m isonitrile and thallium-201 activity are comparable following 3 hours of low flow ischemia [Abstract]. *J Am Coll Cardiol* 1990;15:8A.
45. Sinusas AJ, Bergin JD, Edwards NC, et al. Comparison of Tc-99m methoxyisobutyl isonitrile and Tl-201 uptake during low flow ischemia [Abstract]. *J Nucl Med* 1990;31:713.

(continued from page 776)

SELF-STUDY TEST ANSWERS

the joints of one hand and wrist, while sparing the opposite hand. Furthermore, the blood-pool image will demonstrate selectively greater hyperemia in the joint synovia, which is not seen in this patient.

Pseudogout or CPPD crystal deposition disease is predominantly an ailment of the large joints, such as the knee, usually afflicting one joint initially and rarely the interphalangeal joints. Blood-pool imaging will demonstrate the inflamed synovial vasculature, as in rheumatoid arthritis.

An arteriovenous fistula will lead to short-circuiting of the blood supply to the tissues distal to it, and would not cause the scintigraphic findings seen in this patient. The diffuse hyperperfusion and hyperemia of the entire hand is inconsistent with this diagnosis.

References

1. Holder LE, MacKinnon SE. Reflex sympathetic dystrophy in the hands: clinical and scintigraphic criteria. *Radiology* 1984;152:517-522.
2. Maurer AH, Holder LE, Espinola DA, Rupani HD, Wilgis EFS. Three-phase radionuclide scintigraphy of the hand. *Radiology* 1983;146:761-775.

ITEM 6: Scintigraphic Findings with Recent Fractures

ANSWER: E

Significant accumulation of ^{111}In leukocytes at the site of a healing fracture does not occur unless there is a complicating osteomyelitis. Mildly increased uptake of ^{111}In leukocytes has been reported to occur in association with callus formation or adjacent myositis ossificans. On bone scintigraphy, hyperperfusion, hyperemia, and marked uptake of ^{99m}Tc MDP on delayed images are typical with recent fracture. The accumulation of ^{67}Ga at new fracture sites is usually increased as well. The relative uptake of ^{67}Ga in the lesion can be as great as that of ^{99m}Tc MDP, and either congruent in distribution or less extensive. This seems to be a function of the amount of callus laid down.

References

1. Kim EE, Pjura GA, Lowry PA, Gobuty AH, Traina JF. Osteomyelitis complicating fracture: pitfalls of ^{111}In leukocyte scintigraphy. *AJR* 1987;148:927-930.
2. Schauwecker DS, Park H-M, Mock BH, et al. Evaluation of complicating osteomyelitis with Tc-99m MDP, In-111 granulocytes, and Ga-67 citrate. *J Nucl Med* 1984;25:849-853.

For further in-depth information, refer to the syllabus pages in Nuclear Medicine Self-Study I.